

# Benchmarking of Industrial Stick-Slip Mitigation Controllers

Ulf Jakob F. Aarsnes, \* Florent di Meglio \*\*  
and Roman J. Shor \*\*\*

\* *International Research Institute of Stavanger (IRIS), Oslo, Norway,  
and DrillWell - Drilling and well centre for improved recovery,  
Stavanger, Norway (e-mail: ujfa@iris.no)*

\*\* *Centre Automatique et Systèmes, Mines ParisTech, Paris, France*

\*\*\* *University of Calgary, Department of Chemical and Petroleum  
Engineering, Calgary, Canada*

---

**Abstract:** The present paper evaluates how three different top-drive feedback controllers influence the occurrence of a stick-slip limit cycle in a rotating drill string. The considered controllers are: 1) The industry standard stiff, high-gain controller, 2) SoftTorque, and, 3) ZTorque. The evaluation is performed as a simulation study on a distributed model of a drill string with a collar section and Coulomb friction as a distributed source term. This model is capable of replicating stick-slip oscillations as caused by the reduction in friction from static to dynamic, and have been shown to yield a good match with field data. The simulation study is summarized as a map for each controller indicating the existence and amplitude of oscillations, parametrized in the key friction parameters.

*Keywords:* Drilling control & automation, Closed-loop control, control system analysis, distributed-parameter systems, motor control

---

## 1. INTRODUCTION

Exploration and production of oil and gas in the deep sub-surface, where hydrocarbon reservoirs are found at depths between 2,000 and 20,000 feet, requires that a narrow borehole, between 4 and 24 inches in diameter, be drilled using a slender drill string through a varied downhole environment and along an often snaking wellpath. Drill string vibrations, and their negative consequences on ROP and equipment, is a well known phenomenon when drilling for hydrocarbons. In particular, the torsional oscillations known as stick slip, which are considered to be the most destructive vibrations, are to be avoided.

Significant literature exists which seeks to explain the incidence of stick slip through various implementations of bit-rock interaction and various complexities of drill string dynamic models. The simplest models impose bit-rock interaction as a discontinuous frictional force at the bit and abstract the drill string as a lumped mass, representing the bottom hole assembly (BHA) inertia, and a torsional spring, representing the drill-string stiffness (Bailey and Finnie, 1960; Dashevskiy et al., 2011). These models may be confounded by using more detailed bit-rock interaction representations or by a higher order model of the drill-string (Leine et al., 2002; Nandakumar and Wiercigroch, 2013), but still assume that stick slip is incided due to the

---

\* This research was financially supported by ConocoPhillips, AkerBP, Statoil, Wintershall and the RCN grant (203525/O30) DrillWell, by European Unions Seventh Framework Programme for research, technological development and demonstration under Marie Curie grant agreement no [608695], and the FRIPRO Mobility Grant Fellowship Programme (FRICON).

non-linearity of the frictional force at the bit. All these models have used to demonstrate the occurrence of the limit cycle which exhibits itself as stick-slip and may be used to various types of stick-slip mitigation controllers, including simple tuned PID controllers (Kyllingstad and Nessjøen, 2009; Runia et al., 2013), impedance matching controllers (Dwars, 2015), H-infinity controllers (Yilmaz et al., 2013), sliding mode controllers (Navarro-Lopez et al., 2007), and others.

### 1.1 Contribution and approach

Previous work has considered the stability of the various stick-slip mitigation controllers, but the effectiveness of these controllers in dealing with along-string friction induced stick-slip on a distributed model has not been evaluated (Kyllingstad, 2017). We extend Kyllingstad's work by comparing the effectiveness of three controllers on mitigating stick slip with the bit off bottom utilizing a verified model. In this paper, we first present a summary of the model along with a field validation example, initially presented by Aarsnes and Shor (2018). We then present the theory behind two classes of stick-slip mitigation controllers and evaluate the stick-slip oscillation amplitude for a range of static and dynamic friction factors. In these cases, drill string and rig parameters are taken from field cases.

## 2. MODEL

### 2.1 Torsional dynamics of drill string

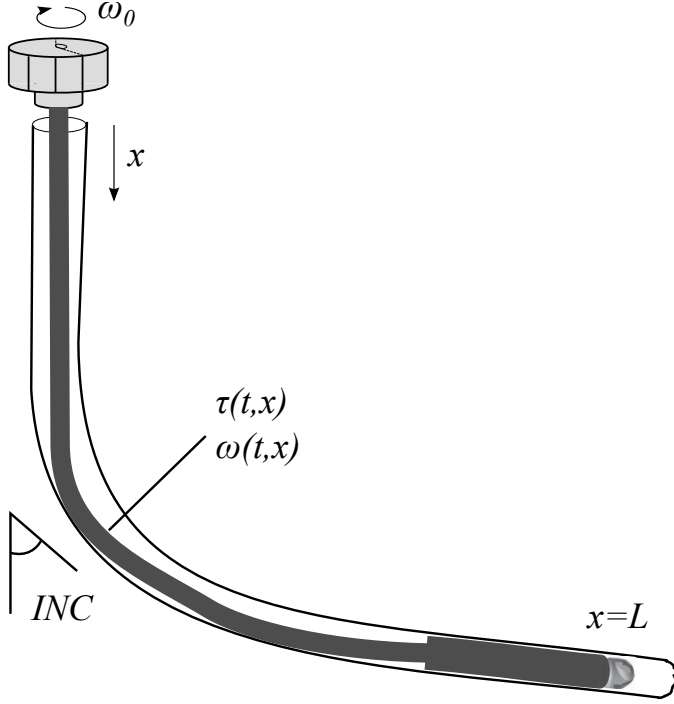


Fig. 1. Schematic indicating the distributed drill string lying in deviate borehole.

We use the distributed model presented by Aarsnes and Shor (2018), similar to Aarsnes and Aamo (2016); Aarsnes and van de Wouw (2018); Germy et al. (2009), which only considers torsional dynamics. That is, for the angular motion, we denote the angular velocity and torque as  $\omega(t, x), \tau(t, x)$ , respectively, with  $(t, x) \in [0, \infty) \times [0, L]$ . The torque is found from shear strain, given as twist per unit length, and letting  $\phi$  denote the angular displacement in the string s.t.  $\frac{\partial \phi(t, x)}{\partial t} = \omega(t, x)$ , we have  $\tau(t, x) = JG(\phi(t, x) - \phi(t, x+dx))/dx$ . Here  $J$  is the polar moment for inertia and  $G$  is the shear modulus. Hence the equations for the angular motion are given by

$$\frac{\partial \tau(t, x)}{\partial t} + JG \frac{\partial \omega(t, x)}{\partial x} = 0 \quad (1)$$

$$J\rho \frac{\partial \omega(t, x)}{\partial t} + \frac{\partial \tau(t, x)}{\partial x} = S(\omega, x), \quad (2)$$

where the source term is due to frictional contact with the borehole and is modeled as

$$S(\omega, x) = -k_t \rho J \omega(t, x) - \mathcal{F}(\omega, x), \quad (3)$$

where  $k_t$  is a damping constant representing the viscous shear stresses between the pipe and drilling mud, and  $\mathcal{F}(\omega)$  is a differential inclusion, to be described, representing the Coulomb friction between the drill string and the borehole.

## 2.2 Discontinuities of multiple sectioned drill string

The lowermost section of the drill string is typically made up of drill collars which may have a great impact on the drill string dynamic due to their added inertia. In particular, the transition from the pipes to collars in the drill string will cause reflections in the traveling waves due to the change in characteristic line impedance Aarsnes and Aamo (2016).

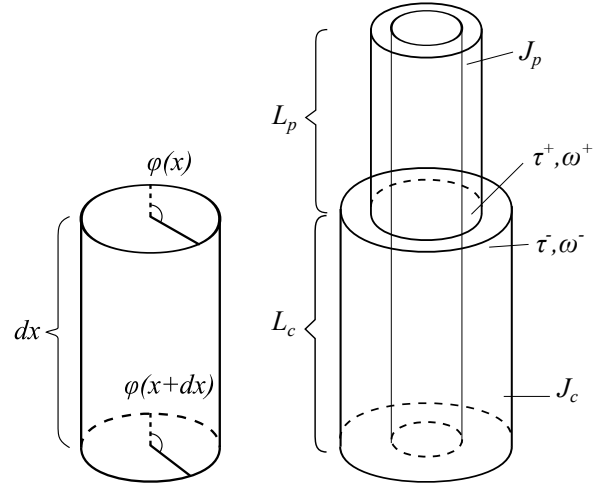


Fig. 2. Infinitesimal drill string element (left) and Collar-Pipe transition (right).

We split the drill string into a pipe section with polar moment of inertia and lengths  $J_p, L_p$  and a collar section with the same parameters given as  $J_c, L_c$ . We use  $\tau^+, \omega^+$  to denote the strain and velocity at the top of the drill collar and  $\tau^-, \omega^-$  at the bottom of the pipe, see Fig. 2. At the transition, the boundary conditions are given by the continuity relations  $\omega^+ = \omega^-$  and  $\tau^+ = \tau^-$ .

## 2.3 Coulomb friction as an inclusion

The Coulomb friction is modeled as an inclusion

$$\begin{cases} \mathcal{F}(\omega, x) = F_c(x) f_{rat}, & \omega > \omega_c, \\ \mathcal{F}(\omega, x) \in [-F_c(x), F_c(x)], & |\omega| < \omega_c, \\ \mathcal{F}(\omega, x) = -F_c(x) f_{rat}, & \omega < -\omega_c, \end{cases} \quad (4)$$

where  $\omega_{threshold}$  is the threshold on the angular velocity where the Coulomb friction transitions from static to dynamic,  $f_{rat} \in [0, 1]$  is the the ratio between the static and dynamics Coulomb friction, and  $\mathcal{F}(\omega) \in [-F_c, F_c]$  denotes the inclusion where

$$\mathcal{F}(\omega, x) = -\frac{\partial \tau(t, x)}{\partial x} - k_t \rho J \omega(t, x) \in [-F_c(x), F_c(x)], \quad (5)$$

and take the boundary values  $\pm F_c(x)$  if this relation does not hold.

To obtain the maximum Coulomb torque function  $F_c(x)$ , we employ the classic Coulomb friction law, which states that the friction opposing a motion horizontal to the plane is proportional to the normal force with the coefficient  $\mu$ . Thus we obtain

$$F_c(x) = \mu \sin(\text{INC}(x)) \rho g A(x) r_o(x), \quad (6)$$

where  $\text{INC}(x)$  is the wellbore inclination,  $g$  is the acceleration of gravity,  $A(x)$  is the cross sectional area of the drill string,  $r_o(x)$  is the outer radius of the drill string. The friction factor  $\mu$  is dependent on the wellbore roughness, mud properties, etc.

Note that the relation (6) is simplistic in that the normal force is affected by other effects than just gravity, with tortuosity being a particular important parameter Menand (2013). Consequently, to compensate for such un-modeled effects, the friction factor  $\mu$  can be tuned (typically in-

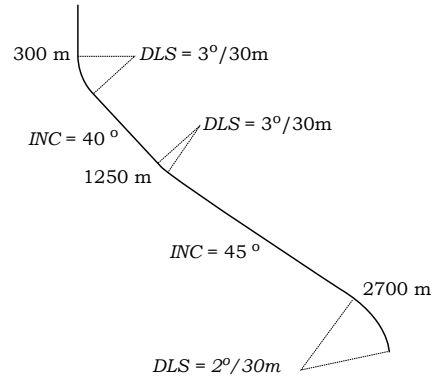
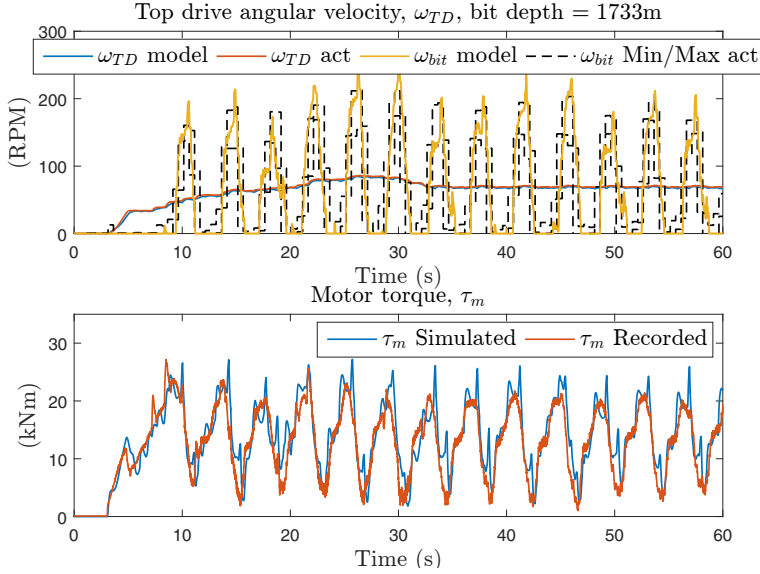


Fig. 3. Recorded and simulated drill-string response at a bit depth of 1,733 m in a well with the survey shown right, using the friction parameters:  $\mu = 0.34$ ,  $f_{rat} = 0.55$ ,  $\omega_c = 19$  (RPM).

creased). As an example, for the case studied by Weijermans et al. (2001), tortuosity was found to increase torque progressively with MD with a 28% increase reported at 17,000 ft when drilled with a RSS with an unwanted dog leg severity of 0.45 and 0.41 deg/100ft in the curve section and the slant section, respectively.

#### 2.4 Boundary conditions

At the topside boundary, the top drive is actuated by a motor torque  $\tau_m$  controlled by a controller, to be designed. The topdrive has the inertia  $I_{TD}$  and hence satisfies the dynamics

$$\frac{\partial \omega_0}{\partial t} = \frac{1}{I_{TD}} (\tau_m - \tau_0), \quad (7)$$

and finally, the angular velocity at the top of the drill string is equal the top drive velocity  $\omega_0$ .

#### 2.5 Model validity

The details of the numerical implementation and a validation of the model is explored by Aarsnes and Shor (2018). Here we illustrate this by briefly considering the *open loop* fit of the model to full scale field data shown in Fig 3. Here the model accurately replicates the stick slip oscillations of the field data. In particular we note that a good replication of the angular BHA velocity.

### 3. FEEDBACK CONTROLLERS

A majority of drilling rigs in the field utilize AC electric top drives controlled using a variety of variable frequency drives – or inverters – which are capable of highly accurate, and often high frequency (> 20 Hz), rotary speed control. A majority of these controllers are simple stiff PI controllers, but two types of stick-slip mitigation controllers are widely deployed – the older SoftTorque / SoftSpeed systems and the newer ZTorque systems.

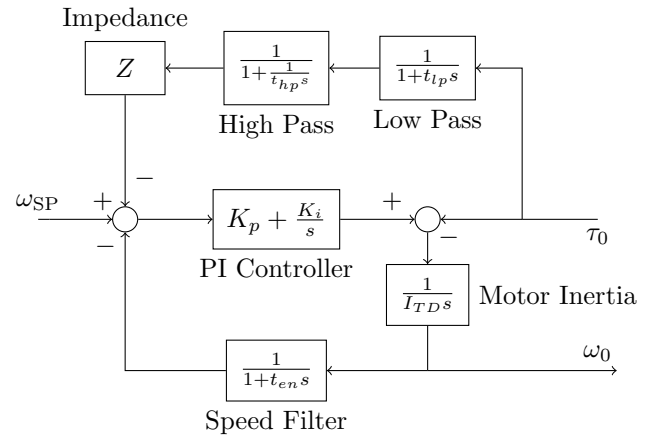


Fig. 4. Control diagram for a ZTorque system with direct pipe torque measurement. For ZTorque  $Z = 1/\zeta_p$  is used. If  $Z = 0$ , the control diagram is equivalent to a SoftTorque or stiff speed controller system.

#### 3.1 Stiff controller

The industry standard controller that is most often used is a high gain PI control to ensure rapid tracking of the top drive set-point. We will also consider this kind of controller for comparisons. The drill pipe impedance is given as  $\zeta_p = J_p \sqrt{G_p \rho}$ , and we will for the stiff controller use the gains

$$K_p = 100\zeta_p, \quad K_i = 5I_{TD}. \quad (8)$$

where  $\zeta_p$  is the characteristic line impedance of the drill string.

#### 3.2 SoftTorque

The current industry standard in handling torsional vibrations are the two products NOV's SoftSpeed (Kyllingstad and Nessjøen, 2009; Halsey et al., 1988) and Shell's Soft-Torque Dwars (2015); Runia et al. (2013). The essential

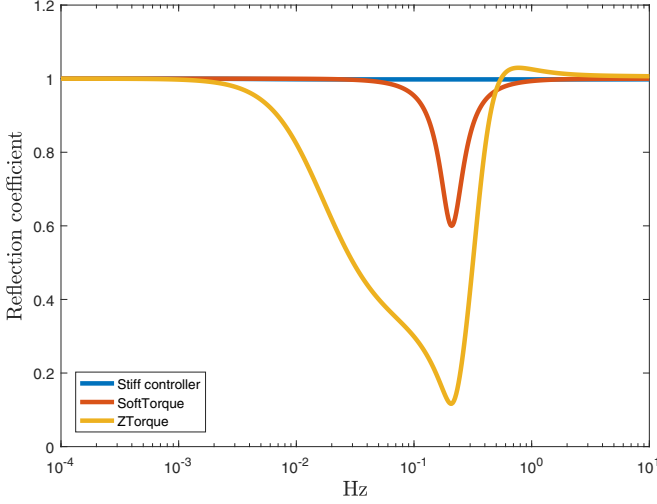


Fig. 5. Topside reflection coefficient of the three considered controllers.

approach of all these solutions is to reduce the reflection coefficient at the top drive in a certain key frequency range (Kyllingstad, 2017).

Assuming for the moment a constant set-point, and defining the controller transfer function  $C(s) \equiv \frac{\tau_m}{\omega_0}$  we obtain the relation:

$$\frac{\tau_0(s)}{\omega_0(s)} = C(s) + I_{TD}s \equiv \bar{C}(s), \quad (9)$$

while the topside reflection coefficient is given as (Kyllingstad and Nessjøen, 2009)

$$R(\omega) = \left| \frac{\bar{C}(s) - \zeta_p}{\bar{C}(s) + \zeta_p} \right|_{s=j\omega}. \quad (10)$$

The approach of SoftSpeed is to set the proportional action to

$$K_p = 4\zeta_p, \quad (11)$$

and then tune the integral gain according to

$$K_i = (2\pi f_c)^2 I_{TD}^2, \quad (12)$$

where  $f_c$  is the frequency (in Hertz) where the minimum of  $R(\omega)$  is achieved. Since the transfer function of an ideal PID controller writes  $C(s) = K_p + \frac{K_i}{s} + K_d s$ , the minimum of the reflection coefficient is obtained at

$$\operatorname{argmin}_{\omega} R(\omega) = \sqrt{\frac{K_i}{I_{TD} + K_d}} \equiv f_c 2\pi. \quad (13)$$

### 3.3 ZTorque

A newer embodiment of stick-slip mitigation control developed by Shell, *ZTorque*, seeks to minimize the reflection coefficient of the top drive for a wider range of frequencies by measuring the torque from between the drill string and top-drive,  $\tau_0$ , and using this in the feedback controller to “artificially” have the top-drive match the impedance of the drill-pipe,  $\zeta_p$ .

For a given pipe torque, the instantaneous top drive rotary velocity necessary to match the pipe impedance is given by, c.f. (7):

$$\omega_0(t) = \frac{1}{\zeta_p} \cdot \tau_0(t) \quad (14)$$

To ensure set point tracking, the control system uses a bandpass filter on the impedance matching rotary velocity – to exclude high frequency noise and low frequency set point changes – by combining a high-pass and low pass filter. Therefore, the PI controller acts on a combination of the tracking error  $\omega_{SP} - \omega_0$ , and the band-pass filtered measured pipe torque  $Z \frac{1}{s + \frac{1}{t_{hp}s}} \frac{1}{s + t_{lp}s} \tau_0$ , i.e. the input to the PI controller is

$$e_{PI} = \omega_{SP} - \omega_0 - Z \frac{s}{(s + \frac{1}{t_{hp}})(1 + t_{lp}s)} \tau_0 \quad (15)$$

where  $t_{hp}, t_{lp}$  are the high pass, low pass filter time constants. Note that the  $\omega_0$  measurement passes through an encoder, illustrated in Fig. 4 as a low-pass filter with time constant  $t_{en}$ . Typically,  $t_{lp}$  and  $t_{en}$  are around 1 to 10 milliseconds and  $t_{hp}$  is around 2 to 10 seconds but must be greater than the period of the first mode of stick-slip. The implementation studied in this paper assumes the presence of a torque sensor between the top drive and drillstring which is capable of real-time measurement of pipe torque,  $\tau_0$ .

In the following we will use a SoftTorque-like controller, (11),(12) and a ZTorque-like controller, (14),(15) to investigate performance of these two types of stick-slip mitigation controllers.

Topside reflection coefficient of the three considered controllers is shown in Fig. 5. The SoftTorque controller uses  $K_p = 4\zeta_p, f_c = 0.2(\text{Hz})$  and the ZTorque controller a 1 ms speed and low pass filters and a 10 second high pass filter.

## 4. SIMULATION STUDY

We consider a rotation startup such as is required after each pipe connection procedure while drilling a well. In this scenario the stationary drill string is initially kept in place by the Coulomb friction until enough torque is built up to overcome it. At which point, pipe-rotation is initiated and the Coulomb friction is reduced as it changes from static to dynamic. The resulting release of the stored energy potentially pushes the drill string into a destructive stick slip limit cycle. Field data examples of this is shown in Fig. 3. We refer to Aarsnes and Shor (2018) for a more detailed description of this phenomena, where it is shown that the simulation model used in the present paper is capable of effectively replicating this type of stick-slip phenomenon.

Figure 7 depicts time series of the bottom rotational velocity and topside torque for two sets of friction parameters  $\mu$  and  $f_{rat}$  in (4), (6). It is clear from these simulations that ZTorque yields a much slower controller, but one that effectively avoids reflections in the relevant frequency range, thus mitigating the tendency of stick slip. The length of time necessary to reach the setpoint rotation speed is directly related to the time constant of the high pass filter in the ZTorque system. It is also clear that the severity of the stick slip, and the tendency of such oscillation to be initiated, is highly dependent on the friction parameters  $\mu, f_{rat}$ . This motivates the creation of the maps indicating the existence and amplitude of oscillations, parametrized in the key friction parameters, in the following.

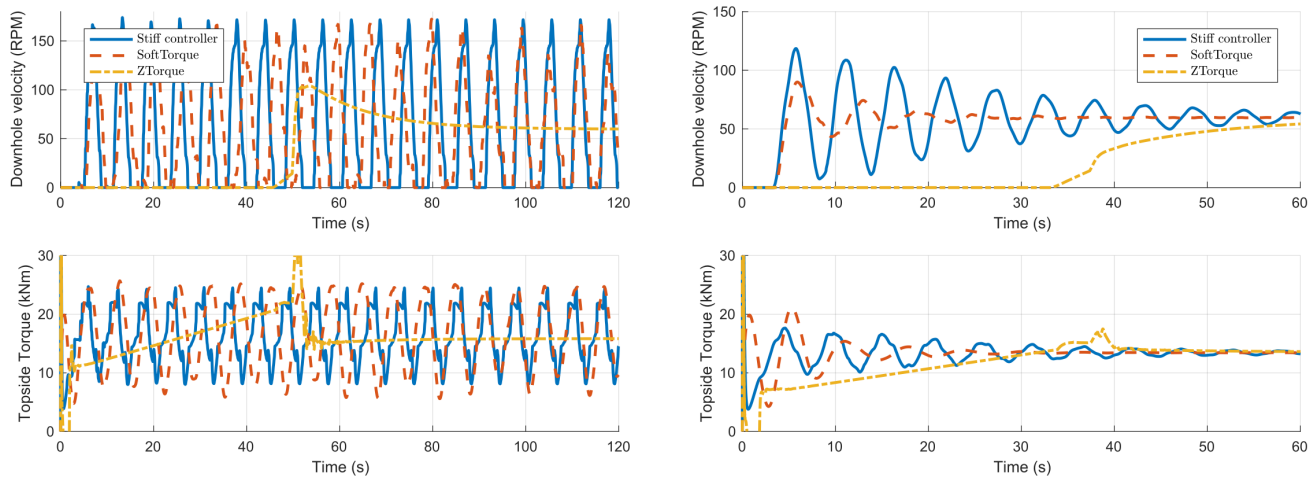


Fig. 6. Bottom velocity (top) and topside torque (bottom) as a function of time, for  $\mu = 0.2$  and  $f_{rat} = 0.75$  (right) and  $\mu = 0.3$  and  $f_{rat} = 0.85$  (left), for each of the three controllers.

Figures 8, 9 and 10 depict maps showing the existence and amplitude of oscillations, parametrized in the key friction parameters, for each of the three controllers, respectively. On each Figure, the color indicates the magnitude in kN of the torque oscillations, given as a function of the Coulomb friction parameters  $\mu$  and  $f_{rat}$  in (4),(6). The blue shaded areas indicate that no limit cycle oscillation is present. These maps have been created by performing the simulation described in the previous paragraph for each set of parameters and then noting the resulting limit-cycle amplitude.

## 5. DISCUSSION AND PERSPECTIVES

The simulation results depicted on Figures 8 and 9 illustrate the fundamentally non-linear property of the stick-slip behavior, and the linearity of the controllers. While the stiff controller fails to prevent the occurrence of stick-slip for a large portion of the map, which seems to indicate a small basin of attraction, it does attenuate the magnitude of the oscillations.

Conversely, the SoftTorque controller features a much larger stable region (i.e., a region where stick slip does not occur), which indicates a larger basin of attraction. However, when the controller fails to avoid the stick-slip oscillations, which then remains away from its equilibrium, the controller tends to increase the magnitude of the oscillations: the controller has an adverse effect along the limit cycle, despite its stabilizing properties close to the equilibrium.

This result stresses the importance of being able to detect stick-slip oscillations when a SoftTorque-like controller is in place, as it is likely to make the oscillations worse. An observer based on the model presented in Section 2.1, able to estimate in real-time the rotational velocity of the drillbit based on topside measurement, will be the topic of future contributions.

A further conclusion is about the effectiveness of the ZTorque controller in removing stick slip oscillations. For the well considered in the present study, the ZTorque

controller avoided stick slip oscillations for the full range of friction parameters  $\mu$  and  $f_{rat}$ . This comes at the costs of, firstly, needing an additional measurement,  $\tau_0$ , secondly, the ability to deliver high instantaneous torque to the top drive to allow for impedance matching through rapid rpm changes, and thirdly, a significantly slower response in rotational velocity of the top-drive. It should be noted that, even though motor torque is seen to be much higher for ZTorque than for the other two controllers, pipe torque is lower.

## REFERENCES

- Aarsnes, U.J.F. and Shor, R.J. (2018). Torsional vibrations with bit off bottom: Modeling, characterization and field data validation. *Journal of Petroleum Science and Engineering*, 163, 712–721. doi: 10.1016/j.petrol.2017.11.024.
- Aarsnes, U.J.F. and van de Wouw, N. (2018). Dynamics of a distributed drill string system: Characteristic parameters and stability maps. *Journal of Sound and Vibration*, 417, 376–412. doi:10.1016/j.jsv.2017.12.002.
- Aarsnes, U.J.F. and Aamo, O.M. (2016). Linear stability analysis of self-excited vibrations in drilling using an infinite dimensional model. *Journal of Sound and Vibration*, 360, 239–259. doi:10.1016/j.jsv.2015.09.017.
- Bailey, J.J. and Finnie, I. (1960). An Analytical Study of Drill-String Vibration. *Transactions of the American Society of Mechanical Engineers*, (May 1960), 122–127.
- Dashevskiy, D., Rudat, J., and Pohle, L. (2011). Model-Based Stability Analysis of Torsional Drillstring Oscillations. In *Proceedings of 2011 IEEE International Conference on Control Applications*. Denver, CO.
- Dwars, S. (2015). Recent Advances in Soft Torque Rotary Systems. In *Proceedings of 2015 SPE/IADC Drilling Conference*, March, 17–19. London, United Kingdom. doi:10.2118/173037-MS.
- Germay, C., Denoël, V., and Detournay, E. (2009). Multiple mode analysis of the self-excited vibrations of rotary drilling systems. *Journal of Sound and Vibration*, 325(1-2), 362–381. doi:10.1016/j.jsv.2009.03.017.
- Halsey, G., Kyllingstad, A., and Kylling, A. (1988). Torque Feedback Used to Cure Slip-Stick Motion. In *SPE*

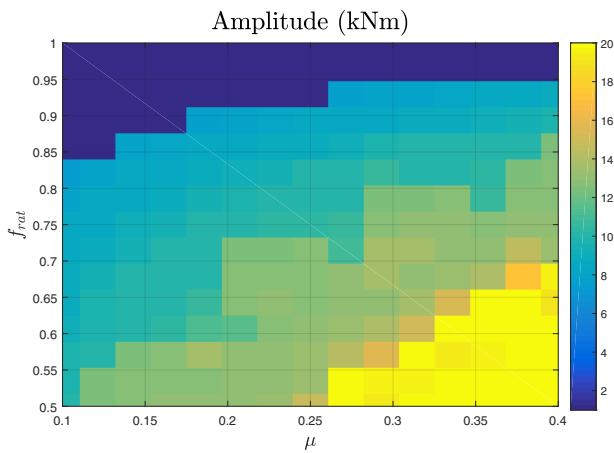


Fig. 7. The stick slip limit cycle amplitude sensitivity with a stiff top drive controller. The blue shaded area indicate that no limit cycle oscillation is present.

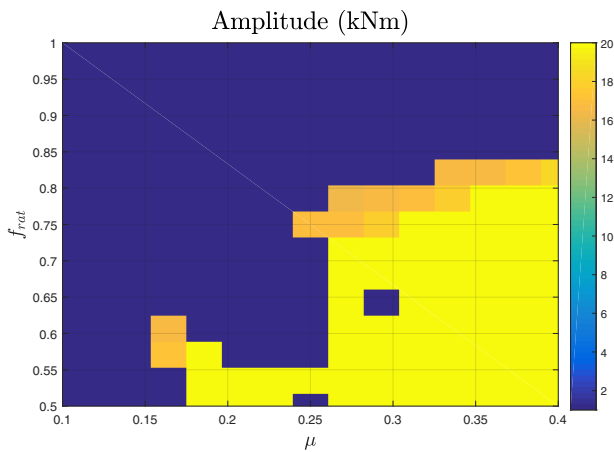


Fig. 8. The stick slip limit cycle amplitude sensitivity with the SoftTorque controller. The blue shaded area indicate that no limit cycle oscillation is present.

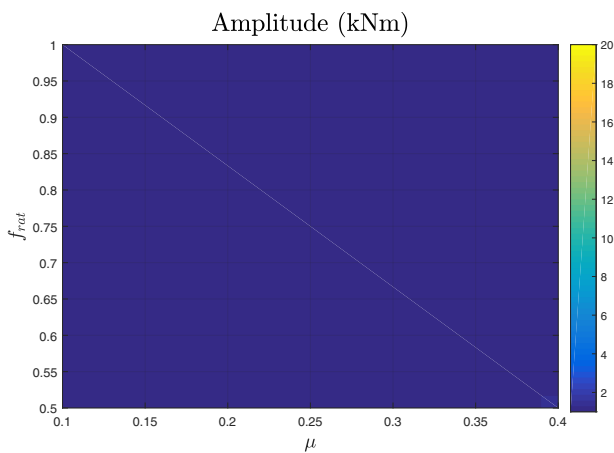


Fig. 9. The stick slip limit cycle amplitude sensitivity with the ZTorque controller. ZTorque effectively avoids stick slip over all considered parameter values.

Annual Technical Conference and Exhibition, 277–282. Society of Petroleum Engineers. doi:10.2118/18049-MS.

Kyllingstad, A. (2017). A Comparison of Stick-Slip Mitigation Tools. In *SPE/IADC Drilling Conference and Exhibition*, March, 14–16. Society of Petroleum Engineers. doi:10.2118/184658-MS.

Kyllingstad, Å. and Nessjøen, P.J. (2009). A New Stick-Slip Prevention System. In *Proceedings of SPE/IADC Drilling Conference and Exhibition*, March, 17–19. doi:10.2118/119660-MS.

Leine, R.I., van Campen, D.H., and Keultjes, W.J.G. (2002). Stick-slip Whirl Interaction in Drillstring Dynamics. *Journal of Vibration and Acoustics*, 124(2), 209. doi:10.1115/1.1452745.

Menand, S. (2013). AADE-13-FTCE-21 Borehole Tortuosity Effect on Maximum Horizontal Drilling Length Based on Advanced Buckling Modeling. In *AADE National Technical Conference and Exhibition*. Oklahoma.

Nandakumar, K. and Wiercigroch, M. (2013). Stability analysis of a state dependent delayed, coupled two DOF model of drill-string vibration. *Journal of Sound and Vibration*, 332(10), 2575–2592. doi:10.1016/j.jsv.2012.12.020.

Navarro-Lopez, E.M., Cort, D., and Cortes, D. (2007). Sliding-mode control of a multi-DOF oilwell drillstring with stick-slip oscillations. In *Proceedings of the 2007 American Control Conference*, 3837–3842. IEEE, New York City. doi:10.1109/ACC.2007.4282198.

Runia, D.J., Dwars, S., and Stulemeijer, I.P.J.M. (2013). A brief history of the Shell "Soft Torque Rotary System" and some recent case studies. In *SPE/IADC Drilling Conference*, 69–76. Society of Petroleum Engineers. doi:10.2118/163548-MS.

Weijermans, P., Ruzska, J., Jamshidian, H., and Matheson, M. (2001). Drilling with Rotary Steerable System Reduces Wellbore Tortuosity. In *SPE/IADC Drilling Conference*. Society of Petroleum Engineers. doi:10.2118/67715-MS.

Yilmaz, M., Mujeeb, S., and Dhansri, N.R. (2013). A H-infinity control approach for oil drilling processes. *Procedia Computer Science*, 20, 134–139. doi:10.1016/j.procs.2013.09.251.